Folding of Long Multiblock Copolymer (PI-*b*-PS-*b*-PI)$_n$ Chains Prepared by the Self-Assembly Assisted Polypolymerization (SAAP) in Cyclohexane

Liangzhi Hong,[†] Fangming Zhu,*[,‡] Junfang Li,[§] To Ngai,[†] Zuowei Xie,[†] and Chi Wu*[,†,§]

Department of Chemistry, The Chinese University of Hong Kong, Shatin, N. T., Hong Kong, Institute of Polymer Science, School of Chemistry and Chemical Engineering, Sun Yat-Sen University, Guangzhou, Guangdong, 510275, China, and The Hefei National Laboratory of Physical Science at Microscale, Department of Chemical Physics, University of Science and Technology of China, Hefei, Anhui, 230026, China

Received September 15, 2007; Revised Manuscript Received January 2, 2008

ABSTRACT: The formation of polymeric micelles made of A−B−A triblock chains in a solvent selectively poor for the middle B-block concentrate and exposes two active end groups so that short triblock chains can be effectively coupled together to form a long (A−B−A)$_n$ multiblock chain with a controllable block length and sequence. Using this method, we successfully prepared a (PI-*b*-PS-*b*-PI)$_{30}$ multiblock copolymer, starting from a triblock PI-*b*-PS-*b*-PI copolymer ($M_n = 4.8 \times 10^4$ g/mol). The coupling efficiency with and without the self-assembly was compared. The folding of such long multiblock chains ($M_n = 1.4 \times 10^6$ g/mol) in a dilute solution (10^{-5} g/mL) was studied by a combination of static and dynamic laser light scattering. The results reveal that such long multiblock chains do not collapse into single-chain globule in a dilute solution even when the solution temperature is much lower than the Θ temperature. Instead, each PS block collapses into a small globule stabilized by the two attached PI blocks on the chain backbone to form a string of coils and beads so that the multiblock chain becomes thicker with an extended conformation without interchain or intrachain association, which is completely different for the association of initial triblock PI-*b*-PS-*b*-PI chains in a selective solvent, i.e., the formation of polymeric micelles.

Introduction

Block copolymers have attracted much attention in both polymer chemistry and physics due to their synthetic challenges, rich phase diagrams and some potential applications.[1−12] The preparation of well-defined block copolymers requires a chain-growth mechanism without any premature chain transfer or termination.[13] Living polymerization, especially living anionic polymerization (LAP), is the most powerful tool for the preparation of well-defined block copolymers with few designed blocks. In principle, one could sequentially add different types of monomers into a living system to prepare a multiblock copolymer. In reality, each addition of new monomer will inevitably terminate some of living chains because of a trace amount of impurities. Another limitation of the sequential addition is that each block with a living end must be sufficiently reactive to initiate the next added comonomer. For example, polystyryllithium can initiate the polymerization of 4-vinylpyridine to form a PS-*b*-P4VP diblock copolymer, but a living P4VP chain cannot further initiate the polymerization of styrene. This is why the sequential addition has been used to prepare copolymers with few blocks, typically diblock and triblock chains.[14]

Alternatively, one could prepare multiblock copolymers by directly coupling different blocks with two reactive end groups, like the step-growth polymerization.[15−17] Preparation of polyurethane is a typical example. However, it should be noted that such a coupling reaction for long initial blocks is extremely ineffective, especially when they are longer than the entanglement length because most of the reactive ends are wrapped and hidden inside the coiled chains in a good solvent.[18] In addition, the concentration of active ends is too low to have a reasonable reaction rate. The increase of polymer concentration results in more active ends, but the solution becomes too viscous to be stirred during the reaction. Up to now, it still remains a challenge to synthesize long multiblock heteropolymer chains with a controllable block length and sequence.

Previously, we proposed a method of using the self-assembly A−B−A triblock chains with two active ends in a selective solvent to assist the preparation of long multiblock copolymer chains with a controllable block length and sequence (SAAP).[18−20] In this method, the self-assembly *concentrates* and *exposes* the two functional end groups on the periphery of the resultant micellelike structure so that they can be effectively coupled together. In the past studies, the yield of SAAP is fairly low and most of the resultant copolymer chains contain only two triblock chains, i.e., (A−B−A)$_2$. In the current study, we have improved several key steps, namely: (1) a high-degree end-functionalization of living triblock chains; (2) a proper choice of the selective solvent; (3) the use of a highly reactive linking agent.

The narrowly dispersed triblock chains prepared in living anionic polymerization can be terminated with some suitable functional groups,[21−24] which are summarized in Table 1. Among them, the carboxylation *via* the addition of CO_2 is a classic and effective method to prepare some end-functionalized polymers because the termination can quantitatively proceeds in THF at −78 °C.[25,26] In this study, we first carboxylated the

* Corresponding authors. The Hong Kong address should be used for all correspondence.
[†] Department of Chemistry, The Chinese University of Hong Kong.
[‡] Institute of Polymer Science, School of Chemistry and Chemical Engineering, Sun Yat-Sen University.
[§] The Hefei National Laboratory of Physical Science at Microscale, Department of Chemical Physics, University of Science and Technology of China.

10.1021/ma702079j CCC: $40.75
Published on Web 02/19/2008

Table 1. Summarization of Literature Information about the Capture of Living Ends of Polymer Chains with Active Functional Groups in Living Anionic Polymerization

functional group	additives
−OH	ethylene oxide;[27,28] styrene oxide;[29] ω-(*tert*-butyldimethylsiloxyl)-α-haloalkanes[30]
−COOH	carbon dioxide;[25,26,31−33] 4-bromo-1,1,1-trimethoxybutane[34]
−Br or −Cl	α,ω-dihaloalkanes[35]
−SH	*tert*-butyldimethylsilyl-3-chloropropyl sulfide;[30] ethylene sulfide, propylene sulfide[36]
−C≡CH	ω-trimethylsilylethynyl-α-haloalkane[23]
$-NH_2$	methoxyamine/methyllithium;[37] ω-(2,2,5,5-tetramethyl-1-aza-2,5-disilacyclopentyl)-α-haloalkanes[38]

two ends of triblock PI-*b*-PS-*b*-PI chains and then assemble them in *n*-hexane, a selective solvent for the PI blocks, to form a core−shell micellelike structure. Hexamethylenediamine (HDA) was used to couple two −COOH end groups on the micelle's periphery in the presence of 1,3-dicyclohexylcarbodiimide (DCC). The coupling efficiency with and without the self-assembly was compared. Then, the carboxylic acid group was further converted to an acyl chloride group to increase its reactivity with HDA or *N,N′*-dimethyl-1,6-hexanediamine (DMHDA). Finally, long 90-block copolymer $(PI\text{-}b\text{-}PS\text{-}b\text{-}PI)_{30}$ chains with a sufficient yield (>∼50%) were successfully prepared. The main objective of the current study is the folding of individual multiblock $(PI\text{-}b\text{-}PS\text{-}b\text{-}PI)_{30}$ chains in a dilute solution. We have chosen cyclohexane as the solvent because it is a good solvent for the PS block at higher temperatures, but a poor solvent at temperatures lower than ∼34 °C. On the other hand, cyclohexane remains a good solvent for the PI block in the temperature range studied.

Experimental Section

Materials. *n*-Butyllithium (1.6 M in hexanes, Acros), dibutylmagnesium (1.0 M in heptanes, Aldrich), 1,3-dicyclohexylcarbodiimide (DCC) (99%, Aldrich) and high purity grade carbon dioxide (>99.9%, Hong Kong Oxygen) were used as received. The purification of monomers and solvents were carried out using previously reported procedures with some slight modification as follows.[39−42] Styrene (≥99%, 10−15 ppm 4-*tert*-butylcatechol inhibitor, Sigma-Aldrich) was dried over finely grounded CaH_2 for 2 days and then fractionally distilled into a flask where a solution of dibutylmagnesium had been vacuum-dried first. It stood at ∼25 °C with continuous stirring until a bright yellow-greenish color was developed. Further, styrene was fractionally distilled into a monomer ampule and about 3 times of purified THF was fractionally distilled into the monomer ampule to form a styrene solution. Isoprene (99%, Acros) was dried over finely grounded CaH_2 for 2 days and then was fractionally distilled into a flask where a solution of *n*-BuLi had been vacuum-dried first. It was stirring with *n*-BuLi for 1 h at 0 °C and then was fractionally distilled into a monomer ampule. Further, three times that amount of purified THF was fractionally distilled into the monomer ampule to form an isoprene solution. Naphthalene (99%, Scharlau) and hexamethylenediamine (HDA) (99%, Panreac) were purified by vacuum sublimation. Thionyl chloride (>99%, Merck) was twicely purified by fractional distillation. *N,N′*-Dimethyl-1,6-hexanediamine (DMHDA) (98%, Aldrich) was twicely purified by fractional distillation in the presence of CaH_2. The HDA and DMHDA were, respectively, dissolved in purified THF. Triethylamine (TEA) (>99%, Scharlau) was refluxed with 4-toluenesulfonyl chloride (>98%, Merck) to remove traces of primary and secondary amines, and then fractionally distilled into a monomer ampule in the presence of CaH_2. THF was refluxed with sodium metal for 2 days before it was fractionally distilled into a solvent ampule with a Rotaflo stopcock in the presence of potassium naphthalenide. *n*-Hexane was first purified by a general procedure[43] and then fractionally distilled into a reaction flask in the presence of *n*-BuLi. Potassium naphthalenide was prepared by the reaction of naphthalene with a slightly excess amount of potassium metal in THF and unreacted potassium metal was removed by a sintered glass filter in vacuum.[44]

Synthesis of PI-*b*-PS-*b*-PI with Two —COOH Ends. HOOC−PI-*b*-PS-*b*-PI−COOH triblock copolymer was synthesized using a high-vacuum line. The conventional break-seal connector was replaced by a newly designed connector, as shown in Figure 1. The detail of living anionic polymerization can be found elsewhere.[39,40,42,45] For the benefit of some readers, we outline it as follows. Sequential anionic polymerization of styrene (2.90 g in THF, 1 h) and isoprene (3.81 g in THF, 2 h) was initiated by potassium naphthalenide (1.30 mL of THF solution, 2.15×10^{-4} mol/mL) in THF (200 mL) at −78 °C under high vacuum. The characteristic orange-yellow color of polyisoprenyl carbanion disappeared immediately when CO_2 was introduced into the reaction mixture at the end of the polymerization.[26,31,33] Before CO_2 was introduced, a portion of the solution was isolated and separately terminated with degassed methanol so that two identical triblock copolymers with and without two −COOH functional end groups were prepared. The copolymers were precipitated in methanol and then filtered and dried in a vacuum at 40 °C. The copolymer was further dissolved in 150 mL of dichloromethane and then washed with 100 mL HCl aqueous solution (pH = 1.0) and a large quality of deionized water before it was precipitated in methanol and dried in a vacuum.[32]

Self-Assembly Assisted Polypolymerization (SAAP). Figure 2 schematically shows the SAAP principle. In comparison with our previous studies, we changed the functional end groups and the linking agent in this study to increase the coupling efficiency. The triblock copolymer with two −COOH end groups is not completely soluble in *n*-hexane, a solvent selectively good for polyisoprene, because of possible interchain hydrogen bonding between the −COOH end groups. We had to add few drops of THF to weaken the hydrogen bonds and make the self-assembly in *n*-hexane possible. After the formation of the core−shell micellelike structures, the solution of DCC in THF was added. The solution mixture was stirred at ∼25 °C for 24 h before the solution of HDA in THF was added to initiate the coupling reaction.

The $(PI\text{-}b\text{-}PS\text{-}b\text{-}PI)_n$ multiblock copolymer was further prepared by coupling α,ω-diacyl chloride end-capped PI-*b*-PS-*b*-PI triblock copolymer (ClOC−PI-*b*-PS-*b*-PI−COCl) chains with diamine. Before the coupling reaction, the ClOC−PI-*b*-PS-*b*-PI−COCl chains were freshly prepared as follows. After HOOC−PI-*b*-PS-*b*-PI−COOH was dissolved in benzene, an excess amount of thionyl chloride and a drop of DMF were added. The solution mixture was stirred at ∼25 °C for 24 h. A small portion of the solution was taken out at different time intervals, and the reaction between thionyl chloride and HOOC−PI-*b*-PS-*b*- PI−COOH was characterized by ^{1}H NMR. A stoichiometric amount of triethylamine was added to absorb the side product (HCl). After removing benzene and unreacted thionyl chloride by vacuum, *n*-hexane was directly distilled into the reaction vessel. ClOC−PI-*b*-PS-*b*-PI−COCl chains can form the core−shell micelles in pure *n*-hexane because its end groups form no hydrogen bond. The solution of *N,N′*-dimethyl-1,6-hexane-diamine (DMHDA) in THF was added to couple the acyl chloride end groups together. Note that the amide group of DMHDA with only one active hydrogen atom was chosen to avoid a possible cross-linking reaction during the coupling. After the coupling reaction, the reaction solution was precipitated in methanol in order to harvest the copolymers.

Characterization of Copolymers. A commercial LLS spectrometer (ALV/DLS/SLS-5022F) equipped with a multi-τ digital time correlator (ALV5000) and a cylindrical 22 mW He−Ne laser

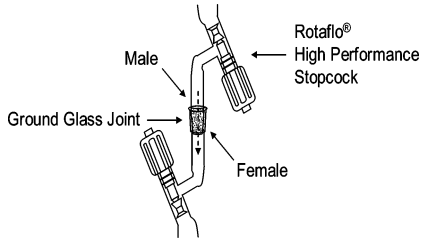

Figure 1. Design of a connector to replace a conventional break-seal joint in high-vacuum anionic polymerization, where two high performance Rotaflo stopcocks are connected by a ground glass joint.

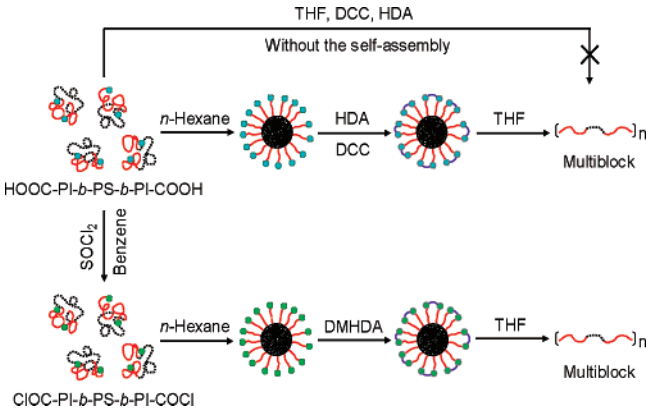

Figure 2. Schematic of coupling PI-*b*-PS-*b*-PI triblock copolymer chains with two active end in a solvent selectively good for PI (self-assembly assisted polypolymerization, SAAP) and in a good solvent for both PS and PI (no self-assembly).

(λ_0 = 632 nm, Uniphase) as the light source was used. In static LLS,[46,47] we can obtain the weight-average molar mass (M_w) and the *z*-average root-mean square radius of gyration ($\langle R_g \rangle_z$) of scattering objects in a dilute solution/dispersion from the angular and concentration dependence of the excess absolute scattering intensity (Rayleigh ratio $R_{vv}(q)$) as

$$\frac{KC}{R_{vv}(q)} \approx \frac{1}{M_w}\left(1 + \frac{1}{3}\langle R_g \rangle q^2\right) + 2A_2C \qquad (1)$$

where $K = 4\pi n^2(dn/dC)^2/(N_A\lambda_0^4)$ and $q = (4\pi n/\lambda_0)\sin(\theta/2)$ with N_A, dn/dC, n, and λ_0 being the Avogadro number, the specific refractive index increment, the solvent refractive index, and the wavelength of the light in a vacuum respectively. A_2 is the second virial coefficient. $(dn/dC)_{632.8\ nm}$ (25 °C) = 0.149 mL/g in THF, determined by using the Jianke differential refractometer.[48] The value of dn/dC in THF, a good solvent for both PI and PS, can also be calculated on the basis of an additive rule from dn/dC and weight fractions of the PI and PS blocks, i.e., $(dn/dC)_{PI-b-PS-b-PI} = W_{PI}(dn/dC)_{PI} + W_{PS}(dn/dC)_{PS}$. The measured and calculated values of dn/dC agree well. Note that different dn/dC values of the polystyrene and polyisoprene blocks in the solution, M_w and $\langle R_g \rangle$ of the multiblock copolymer obtained in a single solvent by static LLS could be apparent. To overcome this problem, we used the initial triblock copolymer as a standard to make an internal correction since we know its molar mass; namely, we used the ratio of scattering intensities from multiblock and triblock chains with the same copolymer concentration. The scattering angular range used was from 20° to 150°.

In dynamic LLS,[49] the Laplace inversion of each measured intensity−intensity time correlation function $G^{(2)}(q,t)$ in the self-beating mode can lead to a characteristic relaxation-time distribution $G(\tau)$. In this study, the CONTIN program in the correlator was used. For a pure diffusive relaxation, τ is related to the translational diffusion coefficient D by $(1/\tau q^2)_{C\to 0, q\to 0} \to D$. Therefore, $G(\tau)$ can be converted into a transitional diffusion coefficient distribution G(D) or further to a hydrodynamic radius distribution $f(R_h)$ by using the Stokes−Einstein equation, $R_h = (k_BT/6\pi\eta)/D$, where k_B, T, and η are the Boltzmann constant, the absolute temperature, and the solvent viscosity respectively. The cumulant analysis of $G^{(2)}(q,t)$ of a narrowly distributed scattering objects can also result in an average characteristic relaxation time $\langle\tau\rangle$ with a sufficient accuracy.

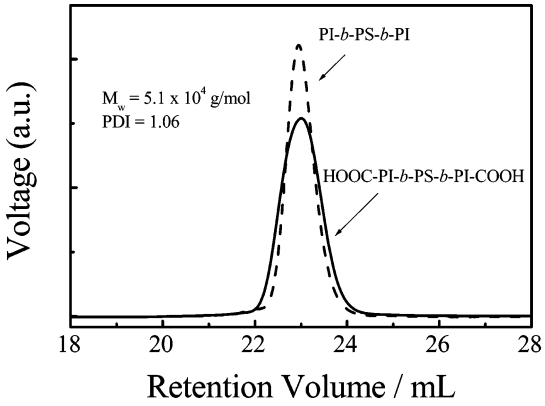

Figure 3. Comparison of SEC profiles of two PI-*b*-PS-*b*-PI triblock copolymers with and without two carboxylic acid end groups in THF.

The size exclusion chromatography (SEC) experiments were conducted at 30 °C by using a SEC-MALLS system consisting of one Waters 1515 isocratic HPLC pump, five Waters UltraStyragel columns (HR2, HR3, HR4, HR5, and HR6), one Waters 2487 dual λ absorbance UV detector, one Wyatt Optilab rEX RI detector, and one Wyatt 18-angle DAWN HELEOS light scattering detector. It can directly measure the molar mass distribution and the radius of gyration of each fraction without a conventional calibration. THF was used as the eluent and the flow rate was 1.0 mL/min. The ^{1}H NMR spectra were recorded in *d*-chloroform at 25 °C with a Bruker DPX 300 MHz NMR spectrometer.

Results and Discussion

Figure 3 shows a comparison of two SEC profiles of PI-*b*-PS-*b*-PI triblock copolymer chains, respectively, terminated with methanol and carbon dioxide. It shows that both of them are narrowly distributed. No interchain coupling occurs during the chain termination. The styrene/isoprene molar ratio determined by ^{1}H NMR is 0.45. The weight fraction of polystyrene (W_{PS}) and polyisoprene (W_{PI}) in this triblock copolymer are 40.8% and 59.2%, respectively. The ^{1}H NMR study also shows that the polymerization of isoprene in THF results in a mixture of ~60% 1,2-addtion and ~40% 3,4-addition.[18] A combination of static LLS, SEC and ^{1}H NMR results shows the −COOH terminated triblock copolymer, HOOC−PI-*b*-PS-*b*-PI−COOH, has the following structure

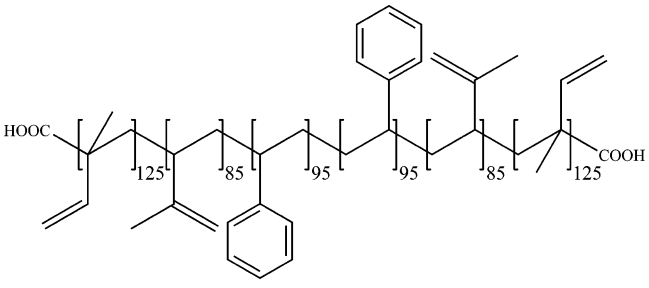

where $M_w = 5.1 \times 10^4$ g/mol and $M_n = 4.8 \times 10^4$ g/mol. The self-assembly of diblock and triblock copolymers in a selective solvent has been well studied.[50−62] In a dilute solution, the insoluble and collapsed blocks normally form a dense core, while the soluble and swollen blocks stay on the periphery to stabilize the self-assembled micellelike structure.

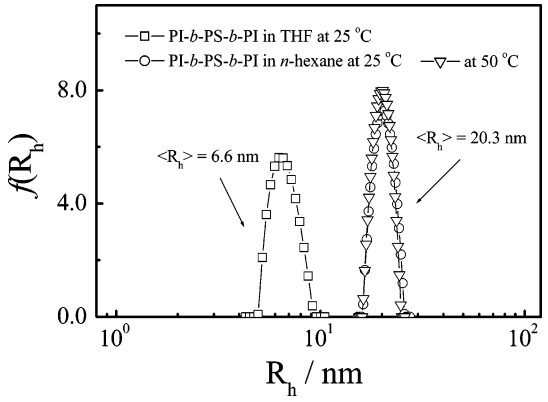

Figure 4. Hydrodynamic radius distributions ($f(R_h)$) of triblock copolymer PI-*b*-PS-*b*-PI chains in THF without the self-assembly as well as in *n*-hexane with the self-assembly at two different temperatures and $\theta = 20°$.

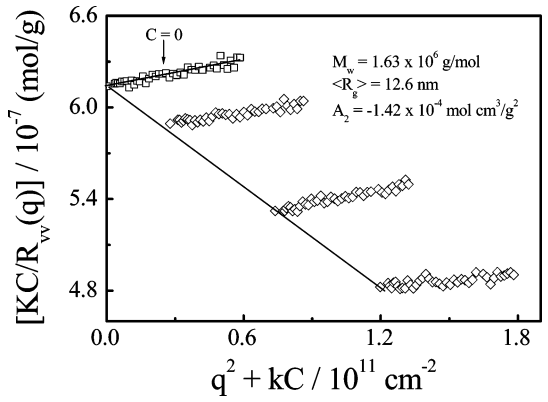

Figure 5. Zimm-plot of triblock copolymer PI-*b*-PS-*b*-PI chains in *n*-hexane, where the copolymer concentration (C) is in the range ($1.11-4.79$) $\times$ 10^{-4} g/mL.

Figure 4 shows a comparison of hydrodynamic radius distributions ($f(R_h)$) of the PI-*b*-PS-*b*-PI chains in different solvents and at different temperatures. It shows that the change of solvent from THF (a good solvent for both PI and PS) to *n*-hexane (a solvent only selectively good for PI) shifts the peak position from ~6−7 nm to ~20 nm. The self-assembled structure, presumably polymeric micelles, is stable in the temperature range 25−50 °C. On the other hand, the average radius of gyration of PI-*b*-PS-*b*-PI micelles in *n*-hexane is 12.6 nm. The ratio $\langle R_g \rangle / \langle R_h \rangle$ is ca. 0.62, lower than 0.774 predicted for a uniform hard sphere. This lower value of $\langle R_g \rangle / \langle R_h \rangle$ can be attributed to the fact that the PS core has a higher chain density than the PI shell.[63] The PI blocks can be visualized as tethered on the PI/PS interface with a stretched conformation due to the chain crowding.[64] Daoud and Cotton,[65] analyzed the tethered layer with a spherical symmetry. Later, Zhulina et al.,[50] showed that the corona thickness (H) is stretched from $aN^{3/5}$ (random coil) to $af^{1/5}N^{3/5}$ by treating it as a star polymer, where a, N, and f are the size of monomer, the degree of polymerization of the soluble block, and the soluble block numbers on the shell, respectively.

Figure 5 shows a typical Zimm-plot of PI-*b*-PS-*b*-PI in *n*-hexane, where the correction of the copolymer concentration (C) by subtracting the critical micelle concentration (cmc) is insignificant because cmc ($\sim 10^{-6}$ g/mL) is rather low. On the basis of eq 1, we can obtain the weight-average molar mass of polymeric micelles ($M_{w,micelle}$) from the intercept of $[KC/R_{vv}(q)]_{q \to 0, C \to 0}$ and then f from 2 $M_{w,micelle}/M_{w,chain}$. The value of f ~ 64 reveals that on average, each PI block in the corona occupies a surface area of ~5 nm^2. The chain extension can be calculated from the ratio of $af^{1/5}N^{3/5}/aN^{3/5}$, i.e., $f^{1/5}$, assuming that the PI blocks are incompressible. Our estimation shows that the stretched PI block in the corona is about twice longer than it is free in a good solvent. The self-assembly concentrates all the functional end groups on the periphery. The stretching of the PI block in the corona helps the functional end groups to stick out so that the coupling reaction is more effective. Recently, a similar idea is also used for thermally reversible binding of cations in an aqueous solution.[66]

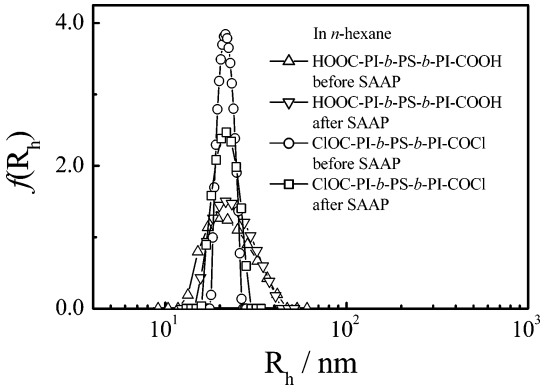

Figure 6. Hydrodynamic radius distributions ($f(R_h)$) of triblock copolymer HOOC−PI-*b*-PS-*b*-PI−COOH chains in *n*-hexane (few drops of THF) and ClOC−PI-*b*-PS-*b*-PI−COCl triblock chains in pure *n*-hexane before and after coupling reaction at $\theta = 20°$.

We found that HOOC−PI-*b*-PS-*b*-PI−COOH is not completely soluble in *n*-hexane. Instead, it forms a cloudy dispersion under stirring. When the stirring stops, the dispersion quickly separates into two cloudy phases. Both of them become clear after half an hour. The top layer is a copolymer solution, while the bottom layer contains a gellike dispersion. It has been known that sufficiently strong interchain interaction between the end groups of polymer chains can lead to the formation of interchain association or even a gel in a dilute solution.[67−73] Addition of few drops of THF can clear the HOOC−PI-*b*-PS-*b*-PI−COOH dispersion, resulting in a stable bluish dispersion. Presumably, THF can preferentially adsorb on the carboxylic acid end groups and weaken the hydrogen bonding. Note that THF was removed in the process of harvesting the reaction products. Figure 6 shows the formation of narrowly distributed HOOC−PI-*b*-PS-*b*-PI−COOH polymeric micelles after the addition of few drops of THF, similar to PI-*b*-PS-*b*-PI in pure *n*-hexane. In contrast, ClOC−PI-*b*-PS-*b*-PI−COCl can form narrowly distributed micelles in pure *n*-hexane because there is no double hydrogen bonding between the two end groups, as schematically shown in the following:

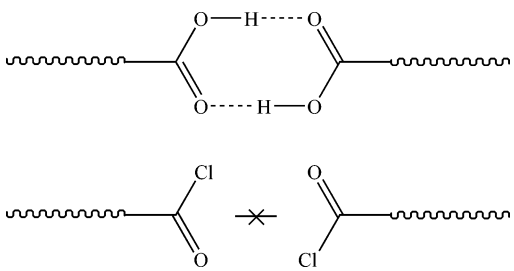

Formation of Multiblock Copolymers. It has been known that a carboxylic acid group can directly and rapidly react with amine to form amide bond in the presence of DCC at room temperature even in water.[44,63,72,74−78] After the self-assembly of HOOC−PI-*b*-PS-*b*-PI−COOH in *n*-hexane, hexamethylenediamine (HDA) was added to couple every two −COOH ends

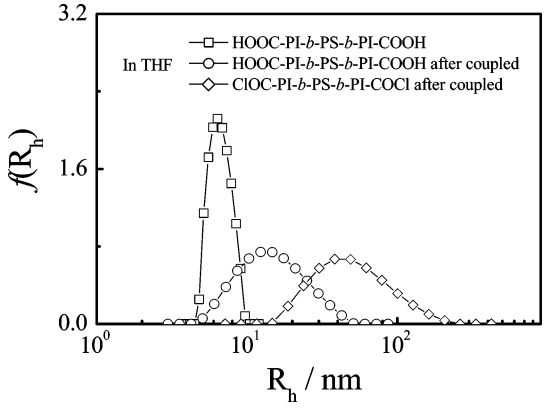

Figure 7. Hydrodynamic radius distributions ($f(R_h)$) of triblock PI-*b*-PS-*b*-PI and multiblock $(PI\text{-}b\text{-}PS\text{-}b\text{-}PI)_n$ copolymer chains in THF at 25 °C and $\theta = 20°$.

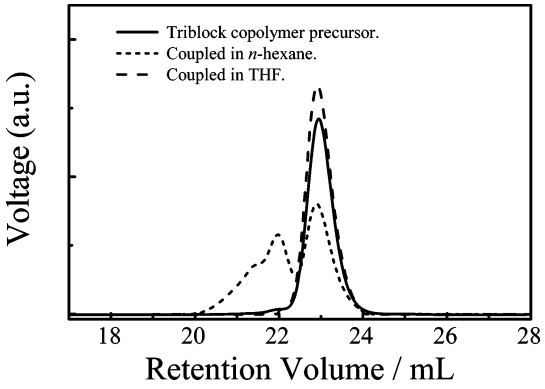

Figure 8. Comparison of SEC profiles of triblock HOOC−PI-*b*-PS-*b*-PI−COOH chains, respectively, after the coupling in THF without the self-assembly and in *n*-hexane with the self-assembly.

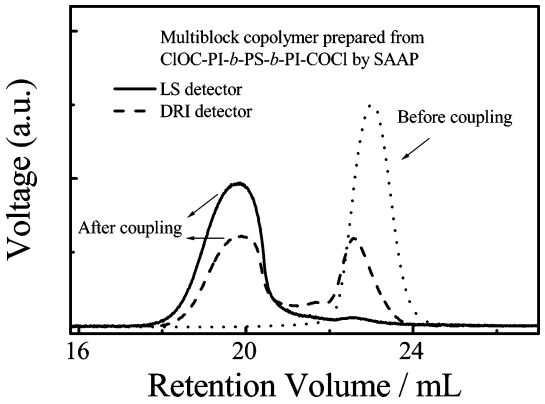

Figure 9. SEC profiles of triblock α,ω-diacyl chloride ClOC−PI-*b*-PS-*b*-PI−COCl chains after the coupling in *n*-hexane with the assistant of the self-assembly.

with the help of DCC. Note that there is always a chance for the intrachain self-coupling. Since the aggregation number is ∼32, i.e., more than 64 −COOH end groups on the periphery, such a self-coupling chance is no more than 2%. Also note that the addition of an insufficient or excessive amount of HDA reduces the coupling efficiency.[18] In order to minimize such a drawback, the linking agent was gradually added. In this study, an equal molar HDA was divided into four portions and each portion was added with a time interval of 24 h. Figure 6 also shows hydrodynamic radius distributions ($f(R_h)$) of the HOOC−PI-*b*-PS-*b*-PI−COOH and ClOC−PI-*b*-PS-*b*-PI−COCl copolymer chains in *n*-hexane after the coupling reaction. It clearly shows that the polymeric micelles remain the same size before and after coupling reaction, indicating that there is no significant intermicelle coupling in the current SAAP.

Figure 7 summarizes hydrodynamic radius distributions of initial triblock copolymers with two different kinds of reactive ending groups, i.e., HOOC−PI-*b*-PS-*b*-PI−COOH and ClOC−PI-*b*-PS-*b*-PI−COCl before and after the coupling reaction. Note that the line-width distribution $G(\Gamma)$ or the distribution of translational diffusion coefficient $G(D)$ obtained in dynamic LLS is intensity weighted. It shows that some of HOOC−PI-*b*-PS-*b*-PI−COOH triblock chains are coupled together so that the average hydrodynamic radius ($\langle R_h \rangle = (k_B T/6\pi\eta)<1/D>$) increases from ∼6−7 to ∼14 nm, while most of the ClOC−PI-*b*-PS-*b*-PI−COCl triblock copolymer chains are coupled together to form long multiblock copolymer chains with a much larger $\langle R_h \rangle$. Therefore, it is much better to use the −COCl end group for the coupling. However, we should note that LLS is not sensitive to short triblock chains when long multiblock chains exist in the solution because the scattering intensity is proportional to the square of mass of a scattering object. In this case, SEC should be a better method to check the SAAP efficiency.

Figure 8 shows that without the self-assembly in THF, there is no visible coupling between HOOC−PI-*b*-PS-*b*-PI−COOH and HDA. As discussed before, this is due to the wrapping of the carboxylic acid end groups inside each coiled triblock chain. On the other hand, the coupling in *n*-hexane with the self-assembly mainly leads to the dimer formation, i.e., $(PI\text{-}b\text{-}PS\text{-}b\text{-}PI)_2$. The coupling efficiency is close to 50%. The small shoulder in the SEC profile on the left side indicates the formation of some long multiblock chains, but the yield is fairly low. Figure 8 reveals that the self-assembly plays a critical role in the coupling of the carboxylic acid ends. It is not surprising to find that only a small amount of long multiblock chains are formed because each carboxylic acid group has to be activated by DCC before it can react with HDA to form an amide linkage. In the reaction mixture, the −COOH and HDA concentrations are so low that the chance of a three-body collision should be rare.

In order to increase the coupling efficiency, we converted each carboxylic acid end group to a highly reactive acyl chloride. In this way, α,ω-diacyl chloride end-capped PI-*b*-PS-*b*-PI chains can be directly coupled by diamine. Further, we simplify the coupling reaction by using the *N*,*N*′-dimethyl-1,6-hexanediamine (DMHDA) with only one active hydrogen as the linking agent instead of HDA to avoid a possibile cross-linking reaction. ^{1}H NMR shows that the reaction between thionyl chloride and HOOC−PI-*b*-PS-*b*-PI−COOH does not alternate the triblock copolymer, but only changes each carboxylic acid group to an acyl chloride.

Figure 9 shows SEC profiles of ClOC−PI-*b*-PS-*b*-PI−COCl before and after the SAAP in *n*-hexane. The comparative study in *n*-hexane and in THF shows that the self-assembly can lead to the formation of long multiblock copolymer $(PI\text{-}b\text{-}PS\text{-}b\text{-}PI)_n$ chains, which can be better viewed when a LLS detector is used because the scattering intensity is proportional to the product of molar mass (M_i) and weight (W_i) of each fraction, while the signal from a differential refractometer is only proportional to W_i. *Note that in each SEC measurement, the initial triblock copolymer chains are used as an internal reference since we know their average molar mass.* Note that we always measure the initial triblock PI-*b*-PS-*b*-PI copolymer before and after the characterization of each resultant multiblock copolymer to make sure that the SEC instrument is stable. Figure 9 also shows that the multiblock copolymer chains are narrowly distributed with

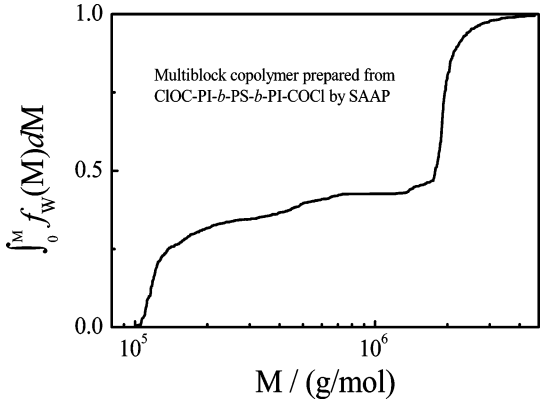

Figure 10. Cumulative weight distribution of triblock ClOC−PI-*b*-PS-*b*-PI−COCl chains after the coupling in *n*-hexane with the assistant of the self-assembly.

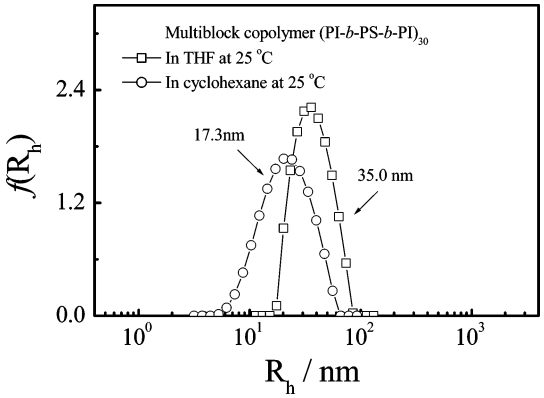

Figure 11. Hydrodynamic radius distributions ($f(R_h)$) of narrowly distributed multiblock copolymer (PI-*b*-PS-*b*-PI)$_{30}$ chains in a good solvent (THF) and in a selective solvent (cyclohexane, a poor solvent for the PS block at 25 °C) and $\theta = 20°$.

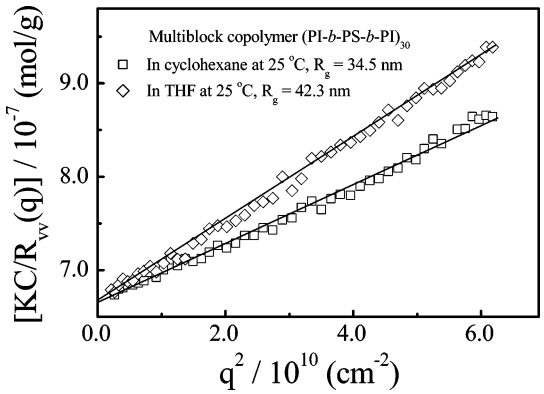

Figure 12. Angular dependence of Raleigh ratio $KC/R_{vv}(q)$ of narrowly distributed multiblock copolymer (PI-*b*-PS-*b*-PI)$_{30}$ chains in a good solvent (THF) and in a selective solvent (cyclohexane, a poor solvent for the PS block at 25 °C).

a number-average molar mass (M_n) of $\sim 1.4 \times 10^6$ g/mol and a polydispersity index (M_w/M_n) of ~1.15.

Figure 10 reveals that with the assistance of the self-assembly, nearly half of the initial triblock copolymer chains are coupled together to form long multiblock copolymer chains. The initial triblock copolymer has an average molar mass of 5×10^4 g/mol. Therefore, each multiblock copolymer chain, on average, contains ~30 initial triblock copolymer chains with a structure of (PI-*b*-PS-*b*-PI)$_{30}$. In a conventional definition, it is a ~90 block copolymer. To the best of our knowledge, the maximum number of blocks in a multiblock copolymer prepared by classical sequential addition living anionic polymerization was no more than 11.[79−81] It should be reminded that the average aggregation number (N_{agg}) of each micelle contains ~32 triblock copolymer chains. Our result indicates that N_{agg} determines the maximum number of triblock copolymer chains in the final multiblock copolymer. In other words, the coupling reaction occurs on the surface of each micelle and most of the triblock copolymer chains inside each micelle are coupled together.

It should be stated that there is always a possibility for two end groups on the same chains to be coupled together to form a cyclic chain. However, the probability is rather low (<2%) because each chain end is on average surrounded by ~60 other chain ends. Our results also confirm it. Otherwise, the coupled copolymer chains would have a much lower molar mass. Another question is whether the resultant multiblock copolymer has an "Olympic" structure, i.e., a set of interlocked rings or microgels. In the SAAP, the middle PS block is insoluble so that individual PS blocks first collapse and then associate together to form a micellelike structure because of two longer soluble PI blocks. We would expect to see such an "Olympic" structure formed in a good solvent instead of a selective solvent. Our results showed that long multiblock copolymer chains do not form inside a good solvent. On the other hand, for a microgellike structure, $\langle R_g \rangle / \langle R_h \rangle$ should be less than one and decreases when it collapses, which is different and opposite what we observed in our current studies.

Figure 10 shows the cumulative distribution of the molar mass of copolymer chains after SAAP. There are two steps in the distribution. The lowest molar mass starts from $\sim 10^5$ g/mol; namely, most of the initial triblock copolymer chains are coupled together. The first step located at $\sim 1.2 \times 10^5$ g/mol, revealing that ~30% of initial triblock copolymer chains are linked together to form dimers, (PI-*b*-PS-*b*-PI)$_2$, presumably due to the intrachain coupling. It suggests that the two end groups of each triblock copolymer chains might not be too far away from each other on the micelle surface. Therefore, the intrachain coupling probability is higher than the expected random coupling probability calculated from the total number of the reactive end groups on the periphery. Finally, *a preparative GPC was used to fractionate the multiblock copolymer* (*PI-b-PS-b-PI*)$_{30}$ *chains from unreacted unimers and small dimers* (*PI-b-PS-b-PI*)$_2$ *after the SAAP*.

The Folding of Long Multiblock Chains in a Dilute Solution. The phase behavior of diblock and triblock copolymer chains in selective solvents has been extensively studied.[82,83] On the other hand, little has been done on the phase behavior of multiblock copolymer chains in solutions except a few theoretical calculations because of the lack of a proper sample.[84]

Figure 11 shows hydrodynamic radius distributions of the narrowly distributed multiblock copolymer chains at 25 °C in THF, a good solvent for both the PS and PI blocks, and in cyclohexane, a good solvent for the PI block and a poor solvent for the PS block at lower temperatures. The average hydrodynamic radius ($\langle R_h \rangle$) shifts from ~35 nm to ~17 nm. Figure 12 shows the angular dependence of the Rayleigh ratio of multiblock copolymer chains, respectively, in THF and cyclohexane at the same temperature. It is known that in static LLS (eq 1), the slope of each line is related to average radius of gyration ($\langle R_g \rangle$) of polymer chains and $\langle R_g \rangle$ is the intensity weighted (*z*) average. The decrease of both $\langle R_g \rangle$ and $\langle R_h \rangle$ indicates the chain contraction in cyclohexane. On the other hand, the extrapolation of $q \rightarrow 0$ leads to the same intercept, indicating that there is no change in M_w. In other words, there is no interchain association. The intercept leads to $M_w = 1.5 \times 10^6$ g/mol. On average, each multiblock copolymer chain contains ~30 PI-*b*-PS-*b*-PI triblock

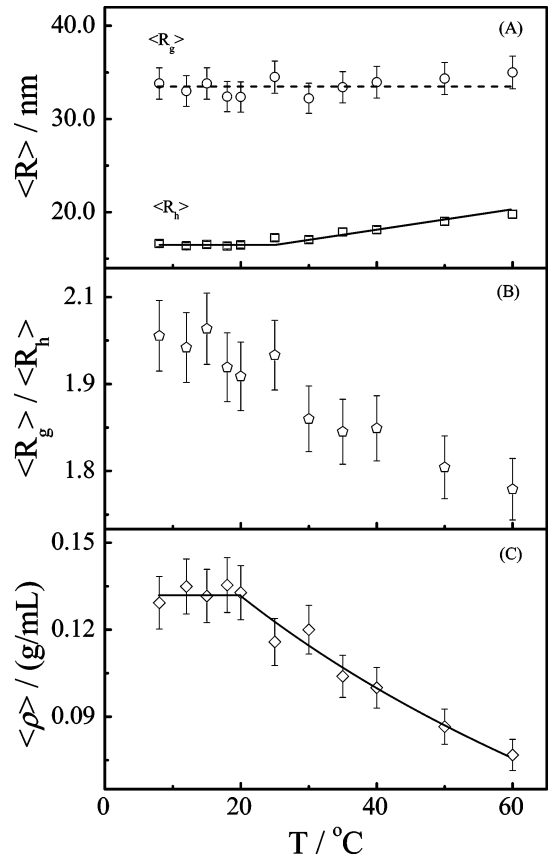

Figure 13. (A) Temperature dependence of average radius of gyration ($\langle R_g \rangle$) and average hydrodynamic radius ($\langle R_h \rangle$) of multiblock copolymer (PI-*b*-PS-*b*-PI)$_{30}$ chains in cyclohexane, a solvent selectively poor for PS at lower temperatures. (B) Temperature dependence of $\langle R_g \rangle / \langle R_h \rangle$ of multiblock copolymer chains in cyclohexane. (C) Temperature dependence of average chain density ($\langle \rho \rangle$) of multiblock chains in cyclohexane, where $\langle \rho \rangle = M_w/(N_A(4/3)\pi\langle R_h \rangle^3]$.

copolymer chains. We ignore the concentration correction because $C \sim 10^{-5}$ g/mL. It is helpful to note that the time-average scattering intensity after the extrapolation to the zero-scattering angle remains a constant in the temperature range 8−60 °C. Therefore, there is no interchain association even at 8 °C at which cyclohexane is a very poor solvent for the PS block. Therefore, Figures 11 and 12 reflect the folding/contraction of individual multiblock copolymer chains in cyclohexane at lower temperatures. It should also be noted that in THF $\langle R_g \rangle / \langle R_h \rangle$ is less than 1.5 predicted for a linear flexible homopolymer chain in a good solvent. However, there is no theory for the overall conformation of a long heteropolymer chain made of alternative blocks with different excluded volumes in a give solvent. One might have to consider ternary interactions. Our current results certainly post a challenge to existing theories.

It was predicted that the folding and contraction of linear $(AB)_n$ multiblock copolymer chains in a selective solvent could result in single-chain micelles or a string of small micelles on the chain backbone, depending on the lengths of the A and B blocks as well as on the total chain length.[84] Figure 13A shows the temperature dependence of $\langle R_g \rangle$ and $\langle R_h \rangle$ of the (PI-*b*-PS-*b*-PI)$_{30}$ multiblock chains in cyclohexane. $\langle R_g \rangle$ remains a constant in the temperature range 8−60 °C, while $\langle R_h \rangle$ only slightly decreases with the temperature and approaches a constant at 25 °C. Note that even at temperatures higher than the UCST of PS in cyclohexane, both $\langle R_g \rangle$ and $\langle R_h \rangle$ of the copolymer chains in cyclohexane are smaller than that in THF, mainly due to the shrinking of the PS blocks. The higher $\langle R_g \rangle / \langle R_h \rangle$ ratio is due to

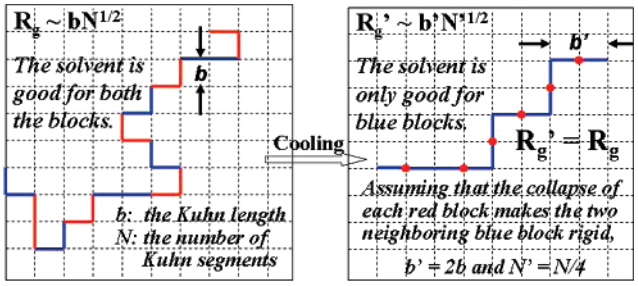

Figure 14. Schematic, qualitative and simplistic explanation of why radius of gyration of a multiblock copolymer chain remains a constant when the red blocks are collapsed into a globule in a poor solvent, where we assume that the globules have no size so that the Kohn length has to be doubled to make R_g a constant.

the fact that the decrease of $\langle R_h \rangle$ is larger than that of $\langle R_g \rangle$. Since the decrease of $\langle R_h \rangle$ is so small and $\langle R_g \rangle / \langle R_h \rangle$ is much high, the formation of a single-flower conformation or the segregation of a number of the collapsed PS blocks to form some micelles on the chain backbone is unlikely. In order to understand how $\langle R_h \rangle$ can decrease, but $\langle R_g \rangle$ remains a constant in the range 60−25 °C, we plot the ratio of $\langle R_g \rangle / \langle R_h \rangle$ vs T, as shown in Figure 13B. It has been well-known that $\langle R_g \rangle / \langle R_h \rangle$ reflects the chain conformation. $\langle R_g \rangle / \langle R_h \rangle = 0.774$ and 1.5, respectively, for a uniform and hard sphere and a linear flexible chain in a good solvent. $\langle R_g \rangle / \langle R_h \rangle$ increases when the chain has an extended conformation.[85−87] Therefore, Figure 13B reveals that as the solution temperature decreases, the PS blocks contract and collapse, but the multiblock copolymer chains become more extended. Figure 13C shows a better view of the contraction of the PS blocks in terms of the average chain density $\langle \rho \rangle$, defined as $M_w/[N_A(4/3)\pi\langle R_h \rangle^3]$.[88] Here, $\langle \rho \rangle$ increases as the solution temperature decrease.

Note that in principle the collapse of the PS blocks should decrease both $\langle R_g \rangle$ and $\langle R_h \rangle$. Figure 14 shows a schematic, qualitative and simplistic explanation of why $\langle R_g \rangle$ of our multiblock copolymer chains nearly remains a constant when one type of blocks (PS, red) collapsed as the solution temperature decreases. Basically, as the solution temperature decreases, the collapse of each PS block into a globule (pearl or bead) makes its two neighboring PI blocks less flexible. The collapse of each PS block makes the chain shorter and decreases the number of the Kuhn segments, but the thickening of the chain (i.e., more rigid) increases the length of each Kuhn segment and makes the chain extended. These two opposite effects somehow cancel each other so that $\langle R_g \rangle$ has not been affected by the temperature. In Figure 14, we assume that each collapsed block has no size and the collapse of the red blocks reduces N by half. In reality, each collapsed block has a size, like a peal or bead, which makes the two blue segments connected to it less flexible; namely, the Kohn length (b) increases. Considering that b is doubled, i.e., N is further reduced by half, we would have $R_g' = (2b)N'^{1/2} = bN^{1/2} = R_g$ so that R_g remains a constant.

More qualitative estimation is as follows: For each PS block (190 monomer units) in a solvent, the average end-to-end distance (R_o) is about 8 nm, corresponding to a radius of gyration of ~3 nm, because each Kuhn segment roughly contains 5 monomer units with a length of about 1 nm.[89] On the other hand, the average diameter of each fully collapsed PS block, estimated on the basis of its molar mass and chain density in the collapsed state, is in the range 6−8 nm, corresponding to a radius of gyration of 2−3 nm.[90] The collapse of each PS block leads to a microphase separation between PI and PS so that the two ends of each PS block will be pulled out by the two soluble

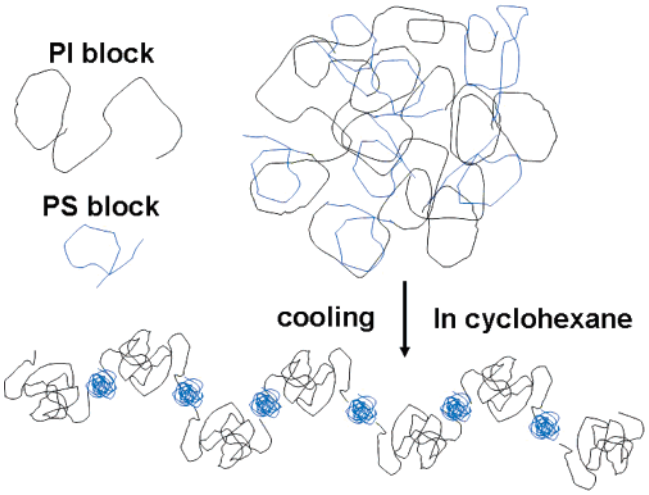

Figure 15. Schematic of conformation change of a multiblock (PI-*b*-PS-*b*-PI)$_n$ chain in cyclohexane, a solvent selectively poor for the PS block at lower temperatures, as the solution temperature decreases.

PI blocks and stay near the periphery of the PS globule. The contraction of each PS block only slightly decreases its end-to-end distance (10−20%).

On the other hand, the two connected PI blocks (420 monomer units) in the multiblock chain have an average end-to-end distance of ∼20 nm. The formation of individual PS globules on the copolymer chain at lower temperatures should increase the end-to-end distance of the PI block because each end is now attached with a 6−8 nm collapsed PS globule. In Figure 14, we assume that the collapsed PS globule have no size. In this case, the Kuhn length of PI should be doubled in order to make $\langle R_g \rangle$ a constant. Considering that each collapsed PS globule is still 6−8 nm, we can safely say that a large change in the Kuhn length of PI is not required to keep $\langle R_g \rangle$ a constant.

Indirectly, the extension of the chain is also supported by the fact that for the same low copolymer concentration (10^{-5} g/mL) used, initial triblock copolymer chains start to undergo interchain association to form micellelike aggregates, but for the multiblock copolymer chains, neither interchain nor intrachain association of the insoluble PS blocks was observed even thought triblock and multiblock copolymer solutions contain the same numbers of PI and PS blocks, i.e., identical chemical composition. Instead, our results suggest that the shrinkage of each PS block results in a more extended pearl-and-string conformation in which each collapsed PS globule is stabilized by the two attached soluble PI blocks, as shown in Figure 15. Note that the centers of mass of all A blocks and of all B blocks are identical and the radii of gyration of all the A blocks and all B blocks are also the same. Therefore, a true $\langle R_g \rangle$ is measured even if scattering of the PI and PS blocks are different. On the other hand, since we used initial triblock copolymer as an internal standard, the measured M_w should also be a true value, indirectly supported by very similar values of M_w obtained respectively in THF and cyclohexane, even thought the salvation of the PS and PI blocks in THF or cyclohexane is likely to be different.

Conclusions

After improving three critical steps in the self-assembly assisted polypolymerization (SAAP), we have successfully coupled 30 triblock copolymer PI-*b*-PS-*b*-PI chains together to form a long 90-block copolymer (PI-*b*-PS-*b*-PI)$_{30}$ with a controllable block length and sequence. These steps are (1) efficiently capturing each end of living triblock A−B−A chains with a highly reactive end group, (2) properly choosing a selective nonsolvent for the middle B-block to lower the critical micellization concentration to minimize individual A−B−A chains in the reaction mixture, and (3) effectively coupling the two active ends with a proper chemistry. The efficiency of coupling initial triblock chains is higher than 50%. The laser light-scattering results reveal that such long multiblock copolymer chains in cyclohexane do not undergo either interchain or intrachain association, like initial triblock copolymer chains, to form polymeric micelles or a single-chain structure (single or multiflowers) even the solvent is very poor for the PS block at lower temperatures. Instead, each insoluble PS block collapses into a small globule (pearl) stabilized by the two attached soluble PI blocks on the chain backbone, just like a string of pearls. Therefore, the chain becomes thicker and more extended. It is expected that such multiblock copolymers would be highly effective as stabilizers if they are amphiphilic and useful as bulk materials if they are made of soft and hard blocks. Moreover, the success of our current study opens a door for further investigation of effects of comonomer composition and distribution on the solution and bulk properties of multiblock copolymer chains, and also leads to some challenge to existing polymer solution theories.

Acknowledgment. The financial support of the Chinese Academy of Sciences (CAS) Special Grant (KJCX2-SW-H14), the National Natural Scientific Foundation of China (NNSFC) Projects (20534020 and 20574065) and the Hong Kong Special Administration Region (HKSAR) Earmarked Project (CU-HK4036/05P, 2160269) is gratefully acknowledged. In addition, we really appreciate some helpful suggestions from Professor M. Schmidt.

Supporting Information Available: Figure S1, showing the scattering vector (q) dependence of apparent diffusion coefficient of multiblock copolymer chains. This material is available free of charge via the Internet at http://pubs.acs.org.

References and Notes

(1) Russell, T. P.; Karis, T. E.; Gallot, Y.; Mayes, A. M. *Nature (London)* **1994**, *368*, 729.
(2) Seul, M.; Andelman, D. *Science* **1995**, *267*, 476.
(3) Zhang, L. F.; Eisenberg, A. *Science* **1995**, *268*, 1728.
(4) Zhang, L. F.; Yu, K.; Eisenberg, A. *Science* **1996**, *272*, 1777.
(5) Jeong, B.; Bae, Y. H.; Lee, D. S.; Kim, S. W. *Nature (London)* **1997**, *388*, 860.
(6) Discher, B. M.; Won, Y. Y.; Ege, D. S.; Lee, J. C. M.; Bates, F. S.; Discher, D. E.; Hammer, D. A. *Science* **1999**, *284*, 1143.
(7) Jenekhe, S. A.; Chen, X. L. *Science* **1999**, *283*, 372.
(8) Discher, D. E.; Eisenberg, A. *Science* **2002**, *297*, 967.
(9) Dubertret, B.; Skourides, P.; Norris, D. J.; Noireaux, V.; Brivanlou, A. H.; Libchaber, A. *Science* **2002**, *298*, 1759.
(10) Savic, R.; Luo, L. B.; Eisenberg, A.; Maysinger, D. *Science* **2003**, *300*, 615.
(11) Li, Z. B.; Kesselman, E.; Talmon, Y.; Hillmyer, M. A.; Lodge, T. P. *Science* **2004**, *306*, 98.
(12) Stoykovich, M. P.; Muller, M.; Kim, S. O.; Solak, H. H.; Edwards, E. W.; de Pablo, J. J.; Nealey, P. F. *Science* **2005**, *308*, 1442.
(13) Lodge, T. P. *Macromol. Chem. Phys.* **2003**, *204*, 265.
(14) Hadjichristidis, N.; Pispas, S.; Floudas, G. A. *Block Copolymers: Synthetic Strategies, Physical Properties, and Applications.* John Wiley & Sons, Inc.: Hoboken, NJ, 2003.
(15) Holder, S. J.; Hiorns, R. C.; Sommerdijk, N.; Williams, S. J.; Jones, R. G.; Nolte, R. J. M. *Chem. Commun.* **1998**, 1445.
(16) Huh, K. M.; Bae, Y. H. *Polymer* **1999**, *40*, 6147.
(17) Lee, J. W.; Hua, F.; Lee, D. S. *J. Controlled Release* **2001**, *73*, 315.
(18) Zhu, F. M.; Ngai, T.; Xie, Z. W.; Wu, C. *Macromolecules* **2003**, *36*, 7405.
(19) Wu, C.; Xie, Z. W.; Zhang, G. Z.; Zi, G. F. *Chin. J. Polym. Sci.* **2001**, *19*, 451.
(20) Wu, C.; Xie, Z. W.; Zhang, G. Z.; Zi, G. F.; Tu, Y. F.; Yang, Y. L.; Cai, P.; Nie, T. *Chem. Commun.* **2002**, 2898.

(21) Szwarc, M. *Nature (London)* **1956**, *178*, 1168.
(22) Morton, M. *Anionic Polymerization: Principles and Practice.* Academic Press: New York, 1983.
(23) Hirao, A.; Hayashi, M. *Acta Polym.* **1999**, *50*, 219.
(24) Jagur-Grodzinski, J. *J. Polym. Sci., Polym. Chem.* **2002**, *40*, 2116.
(25) Ji, H. N.; Nonidez, W. K.; Advincula, R. C.; Smith, G. D.; Kilbey, S. M.; Dadmun, M. D.; Mays, J. W. *Macromolecules* **2005**, *38*, 9950.
(26) Quirk, R. P.; Yin, J.; Fetters, L. J.; Kastrup, R. V. *Macromolecules* **1992**, *25*, 2262.
(27) Karatzas, A.; Talelli, M.; Vasilakopoulos, T.; Pitsikalis, M.; Hadjichristidis, N. *Macromolecules* **2006**, *39*, 8456.
(28) Ji, H. N.; Sato, N.; Nonidez, W. K.; Mays, J. W. *Polymer* **2002**, *43*, 7119.
(29) Quirk, R. P.; Hasegawa, H.; Gomochak, D. L.; Wesdemiotis, C.; Wollyung, K. *Macromolecules* **2004**, *37*, 7146.
(30) Tohyama, M.; Hirao, A.; Nakahama, S.; Takenaka, K. *Macromol. Chem. Phys.* **1996**, *197*, 3135.
(31) Quirk, R. P.; Yin, J.; Fetters, L. J. *Macromolecules* **1989**, *22*, 85.
(32) Pan, J.; Chen, M. F.; Warner, W.; He, M. Q.; Dalton, L.; Hogen-Esch, T. E. *Macromolecules* **2000**, *33*, 4673.
(33) Choi, S. B.; Han, C. D. *Macromolecules* **2003**, *36*, 6220.
(34) Hirao, A.; Nagahama, H.; Ishizone, T.; Nakahama, S. *Macromolecules* **1993**, *26*, 2145.
(35) Hirao, A.; Tohoyama, M.; Nakahama, S. *Macromolecules* **1997**, *30*, 3484.
(36) Quirk, R. P.; Ocampo, M.; Polce, M. J.; Wesdemiotis, C. *Macromolecules* **2007**, *40*, 2352.
(37) Quirk, R. P.; Cheng, P. L. *Macromolecules* **1986**, *19*, 1291.
(38) Ueda, K.; Hirao, A.; Nakahama, S. *Macromolecules* **1990**, *23*, 939.
(39) Fetters, L. J. *J. Res. Natl. Bur. Stand. Phys. Chem.* **1966**, *70*, 421.
(40) Morton, M.; Fetters, L. J. *Rubber Chem. Technol.* **1975**, *48*, 359.
(41) Ndoni, S.; Papadakis, C. M.; Bates, F. S.; Almdal, K. *Rev. Sci. Instrum.* **1995**, *66*, 1090.
(42) Hadjichristidis, N.; Iatrou, H.; Pispas, S.; Pitsikalis, M. *J. Polym. Sci., Polym. Chem.* **2000**, *38*, 3211.
(43) Armarego, W. L. F.; Chai, C. L. L. *Purification of Laboratory Chemicals*, 5th ed.; Butterworth-Heinemann: Oxford, U.K., 2003.
(44) Batra, U.; Russel, W. B.; Pitsikalis, M.; Sioula, S.; Mays, J. W.; Huang, J. S. *Macromolecules* **1997**, *30*, 6120.
(45) Uhrig, D.; Mays, J. W. *J. Polym. Sci., Polym. Chem.* **2005**, *43*, 6179.
(46) Chu, B. *Laser Light Scattering: Basic Principles and Practice*; Academic Press: San Diego, CA, 1991.
(47) Wu, C.; Chu, B. Light Scattering. In *Experimental Methods in Polymer Science: Modern Methods in Polymer Research and Technology*, Tanaka, T., Grosberg, A., Doi, M., Eds.; Academic Press: San Diego, CA, 2000; p 1.
(48) Wu, C.; Xia, K. Q. *Rev. Sci. Instrum.* **1994**, *65*, 587.
(49) Pecora, R. *Dynamic Light Scattering: with Applications to Chemistry, Biology, and Physics*; Dover Publications: New York, 2000.
(50) Birshtein, T. M.; Zhulina, E. B. *Polymer* **1989**, *30*, 170.
(51) Nagarajan, R.; Ganesh, K. *J. Chem. Phys.* **1989**, *90*, 5843.
(52) Halperin, A. *Macromolecules* **1987**, *20*, 2943.
(53) Noolandi, J.; Hong, K. M. *Macromolecules* **1983**, *16*, 1443.
(54) Izzo, D.; Marques, C. M. *Macromolecules* **1993**, *26*, 7189.
(55) Izzo, D.; Marques, C. M. *Macromolecules* **1997**, *30*, 6544.
(56) Leermakers, F. A. M.; Wijmans, C. M.; Fleer, G. J. *Macromolecules* **1995**, *28*, 3434.
(57) Zhulina, E. B.; Adam, M.; LaRue, I.; Sheiko, S. S.; Rubinstein, M. *Macromolecules* **2005**, *38*, 5330.
(58) Forster, S.; Zisenis, M.; Wenz, E.; Antonietti, M. *J. Chem. Phys.* **1996**, *104*, 9956.
(59) LaRue, I.; Adam, M.; Pitsikalis, M.; Hadjichristidis, N.; Rubinstein, M.; Sheiko, S. S. *Macromolecules* **2006**, *39*, 309.
(60) Bang, J.; Jain, S. M.; Li, Z. B.; Lodge, T. P.; Pedersen, J. S.; Kesselman, E.; Talmon, Y. *Macromolecules* **2006**, *39*, 1199.
(61) Riess, G. *Prog. Polym. Sci.* **2003**, *28*, 1107.
(62) Hamley, I. W. *Block Copolymers in Solution: Fundamentals and Applications*; John Wiley & Sons: Chichester, U.K., 2005.
(63) Tu, Y. F.; Wan, X. H.; Zhang, D.; Zhou, Q. F.; Wu, C. *J. Am. Chem. Soc.* **2000**, *122*, 10201.
(64) Halperin, A.; Tirrell, M.; Lodge, T. P. *Adv. Polym. Sci.* **1992**, *100*, 31.
(65) Daoud, M.; Cotton, J. P. *J. Phys. (Paris)* **1982**, *43*, 531.
(66) Custers, J. P. A.; Kelemen, P.; van den Broeke, L. J. P.; Stuart, M. A. C.; Keurentjes, J. T. F. *J. Am. Chem. Soc.* **2005**, *127*, 1594.
(67) Broze, G.; Jerome, R.; Teyssie, P. *Macromolecules* **1982**, *15*, 920.
(68) Davidson, N. S.; Fetters, L. J.; Funk, W. G.; Graessley, W. W.; Hadjichristidis, N. *Macromolecules* **1988**, *21*, 112.
(69) Pispas, S.; Hadjichristidis, N. *Macromolecules* **1994**, *27*, 1891.
(70) Pispas, S.; Hadjichristidis, N.; Mays, J. W. *Macromolecules* **1994**, *27*, 6307.
(71) Hadjichristidis, N.; Pispas, S.; Pitsikalis, M. *Prog. Polym. Sci.* **1999**, *24*, 875.
(72) Liu, S. Y.; Hu, T. J.; Liang, H. J.; Jiang, M.; Wu, C. *Macromolecules* **2000**, *33*, 8640.
(73) Pispas, S.; Allorio, S.; Hadjichristidis, N.; Mays, J. W. *Macromolecules* **1996**, *29*, 2903.
(74) Sheehan, J. C.; Hess, G. P. *J. Am. Chem. Soc.* **1955**, *77*, 1067.
(75) Tang, P. *Org. Synth.* **2005**, *81*, 262.
(76) Kubo, M.; Hayashi, T.; Kobayashi, H.; Tsuboi, K.; Itoh, T. *Macromolecules* **1997**, *30*, 2805.
(77) Pantazis, D.; Schulz, D. N.; Hadjichristidis, N. *J. Polym. Sci., Polym. Chem.* **2002**, *40*, 1476.
(78) Ma, Q. G.; Wooley, K. L. *J. Polym. Sci., Polym. Chem.* **2000**, *38*, 4805.
(79) Wu, L. F.; Cochran, E. W.; Lodge, T. P.; Bates, F. S. *Macromolecules* **2004**, *37*, 3360.
(80) Nagata, Y.; Masuda, J.; Noro, A.; Cho, D. Y.; Takano, A.; Matsushita, Y. *Macromolecules* **2005**, *38*, 10220.
(81) Wu, L. F.; Lodge, T. P.; Bates, F. S. *Macromolecules* **2006**, *39*, 294.
(82) Hanley, K. J.; Lodge, T. P.; Huang, C. *Macromolecules* **2000**, *33*, 5918.
(83) Lodge, T. P.; Pudil, B.; Hanley, K. J. *Macromolecules* **2002**, *35*, 4707.
(84) Halperin, A. *Macromolecules* **1991**, *24*, 1418.
(85) Wu, C.; Qiu, X. P. *Phys. Rev. Lett.* **1998**, *80*, 620.
(86) Siu, M.; Zhang, G. Z.; Wu, C. *Macromolecules* **2002**, *35*, 2723.
(87) Wang, X. H.; Goh, S. H.; Lu, Z. H.; Wu, C. *Macromolecules* **1999**, *32*, 2786.
(88) Siu, M.; Liu, H. Y.; Zhu, X. X.; Wu, C. *Macromolecules* **2003**, *36*, 2103.
(89) Colby, R. H. *J. Polym. Sci., Part B: Polym. Phys.* **1997**, *35*, 1989.
(90) Wu, C.; Zhou, S. *Macromolecules* **1995**, *28*, 8381.

MA702079J